DYNAMICS AND RADIATION OF DIRECT HIGH-CURRENT DISCHARGES IN THE ATMOSPHERE

A. F. ALEKSANDROV, V. V. ZOSIMOV, S. P. KURDYUMOV, Yu. P. POPOV, A. A. RUKHADZE, and I. B. TIMOFEEV

Moscow State University

Submitted April 16, 1971

Zh. Eksp. Teor. Fiz. 61, 1841–1855 (November, 1971)

The results of an experimental investigation into the dynamics of and the radiation emitted by high-current (up to 200 kA) impulsive discharges (duration ~150–200 μsec) produced by the electric explosion of long (75 cm) thin wires in air at atmospheric pressure are presented. The characteristic dimensions, conductivity, and temperature of the discharge plasma, as well as the nature of the spectrum and yield of the radiation in various spectral ranges have been measured. The experimental results are compared with the theory and with the results of computations carried out on an electronic computer. A satisfactory agreement is observed. It is shown that high-current discharges in a dense plasma efficiently converts electrical energy into light energy. Thus, the total yield of radiation in the transparency band of quartz for a discharge in the atmosphere can attain a value of 40 kJ (about 45% of the energy stored in the installation), which is considerably higher than the radiation yield of existing laser pumping tubes.

1. INTRODUCTION

THE appearance in recent years of a large number of papers on the theoretical [1-7] and experimental [1,7-12] study of the dynamics of high-current pulsed discharges in gases and vacuum is due to the possibility of their application as powerful sources of radiation of definite spectral composition, which are necessary for the power pumping of lasers. Naturally, it is desirable here to have for pumping an independent light source which would be suitable for different active media in the gaseous, solid or liquid phase. Such a source can be realized by producing a dense self-constricted discharge, which is separated from the walls of the discharge chamber, i.e., a plasma filament that borders on the vacuum and in which the discharge current performs the function of heating, as well as the function of magnetic confinement of the plasma. In the main, a distinctive feature of such a discharge is, in contrast to the well-studied high-temperature "thermonuclear" pinches (see [13,14] and the literature cited there), the requirement for a higher density and lower plasma temperature, and this leads to a decisive role for radiation in the dynamics and energetics of the discharge, and to the necessity for the effects of the finite conductivity to be taken into account. Such discharges have been studied in detail—theoretically in [1-6] and experimentally in [8-10]. The experimental results exhibit a fairly high efficiency for the discharges as sources of radiation, as well as a good agreement between theory and experiment.

On the other hand, the study of the radiation of high-current discharges, directly produced in a gaseous medium is also an urgent problem, since it might turn out that in a gaseous active medium the most efficient way of pumping would be by means of the production of a discharge directly in that gas. Such a discharge has been theoretically studied on the basis of the equations of hydrodynamics with radiative heat conduction in [7], where their self-similar solutions have been obtained. An experimental verification was carried out in [11]. However, as will be shown below, and as has previously been pointed out, [12] a self-similar solution has a comparatively narrow region of applicability—only for the instants of time when the magnetic pressure of the discharge current can be neglected in comparison with the hydrodynamic pressure of the plasma. For experiments with capacitive energy accumulators, when the discharge circuit has the form of an oscillatory circuit, this condition is usually fulfilled only up to moments of time somewhat smaller than a quarter of its period. The experiments in [11,12] were done on installations with a comparatively small period (15–20 μsec), as a result of which the region of applicability of the self-similar theory was extremely narrow—up to ~3 μsec (for details, see [12]).

In view of this, our investigation of a discharge in the atmosphere was conducted with a circuit with a sufficiently long period, $\tau \gtrsim 100$ μsec. Its theoretical description is given with the aid of numerical computations carried out on an electronic computer. The results obtained are compared with the results of self-similar calculations, which, as will subsequently become apparent, have under our conditions a sufficiently large (with respect to time) region of applicability.

2. DESCRIPTION OF THE EXPERIMENTAL SETUP AND THE MEASUREMENT PROCEDURE

The experimental setup which was used in the present work to investigate high-current discharges in air is a discharge circuit of capacitors of the type IM-50-3. A block diagram of the setup is shown in Fig. 1.

The capacitor bank consisted of two units $C_{1,2}$, each of which had a capacitance of 144 μF and were connected to the load through separate vacuum disk switches $P_{1,2}$ with four floating electrodes. The construction of the discharge gaps is described in [15]. The triggering

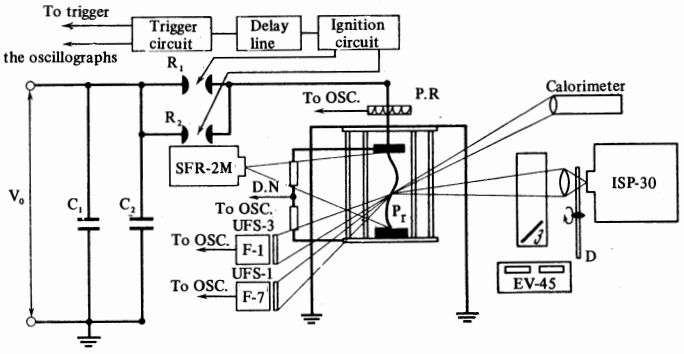

FIG. 1. Block diagram of the experimental setup.

of each discharge tap was accomplished by means of two "spark plugs," which were coaxial plasma injectors. A breakdown of the discharge gaps occurred when a high-voltage pulse, generated by the trigger circuit, was delivered to the candle. The dispersion in the triggering of both discharge gaps did not exceed 0.5 μsec. The bank was hooked up by a coaxial cable of the RK-50-9-11 type. The total stray inductance of the discharge circuit was 300 nH.

The discharge tube consisted of two massive cylindrical electrodes in the form of disks of diameter 130 mm, between which a thin metallic wire, which was used for the initiation of the breakdown of the long discharge gap, was stretched. To reduce the inductance of the discharge tube, the upper electrode was braced by eight brass rods located at equal distances in a circle of diameter 480 mm. These rods served at the same time as the return current conductor and as guide bars for the mobile upper electrode. Such a design made the tube equivalent to a coaxial cable whose length could be varied from zero (a shorted discharge gap) to 90 cm. The rods were connected to a common "ground" of the system, while the lower electrode was connected by means of the discharge gaps to the capacitor bank.

The shape and characteristic dimensions of the discharge were investigated with the aid of SFR-2M ultra-high-speed cameras, the volt-ampere characteristics were measured, and the radiation of the discharge was investigated. The discharge current was measured with a Rogowski loop. The voltage on the tube was measured by means of a noninductive type TVO-10 resistance voltage divider.

The investigation into the nature and magnitude of the absolute yield of radiation was carried out with the aid of methods used earlier in the study of the radiation of high-speed discharges in air and of vacuum discharges,[8-12] hence we restrict ourselves to a brief enumeration of them. The time-scanned spectrum of the radiation was registered by an ISP-30 quartz spectrograph. The time scanning was accomplished with the aid of a rotating disk with slits, located in front of the entrance slit of the spectrograph. The registration of the radiation from the discharge in separate spectral intervals was carried out by means of the oscillography of signals from F-1 and F-7 photocells with light filters. For absolute calibration, a standard source of the type ÉV-45 was used.[16] The integrated radiation energy in the transmission region of quartz was measured by means of a calorimeter.

3. EXPERIMENTAL INVESTIGATION OF THE DYNAMICS AND THE RADIATION OF A LONG DISCHARGE IN AIR

For the initiation of the electrical breakdown of the discharge gap in the present work, we used the explosion of a thin nichrome wire of diameter 0.1 mm. The length of the discharge gap was 75 cm. The experiments were performed for two values of the voltage across the bank: 20 and 24 kV. The stored energy was 58 and 83 kJ respectively.

Figure 2 shows oscillograms of the current and voltage in the discharge gap for an initial voltage of 20 kV. It can be seen from the oscillograms that the nature of the variations of the current and voltage was nearly periodic, but they were strongly damped. The main energy contribution to the discharge apparently occurs in such a situation during the first half-period of the current, equal approximately to 53 μsec. The continuous lines in Fig. 3 are the volt-ampere characteristics of a discharge obtained from the corresponding oscillograms for the first half-period. For the case cited, the maximum am-

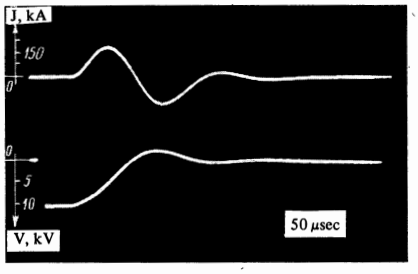

FIG. 2. Oscillogram of a discharge current J and of the voltage drop V across the discharge gap.

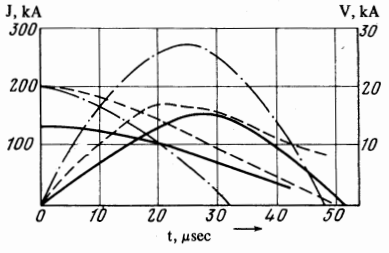

FIG. 3. Dependence of J and V on time for the first half-period. The solid curves are experimental, the dashed and dash-dot curves are the results of electronic computer calculations.

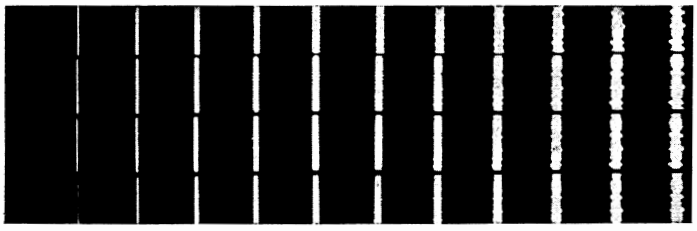

FIG. 4. Typical streak photograph of a discharge. The time interval between the frames is 1 μsec.

plitude of the current was 145 kA, while the maximum value of the voltage across the gap was ~13 kV. For an initial voltage of 24 kV, the maximum value of the voltage across the discharge gap was ~20 kV, while the maximum value of the strength of the discharge current was 195 kA. It follows from the shape of the volt-ampere characteristics that under the conditions of the experiment, the stray inductance of the discharge circuit was commensurable with the inductance of the discharge.

Figure 4 shows a typical streak photograph of a discharge. As can be seen, there is at the initial stage a well-defined layered (stratified) structure of the discharge channel which is typical of an electrical explosion of conductors.[17,18] The stratification disappears in approximately 5–6 μsec, and the discharge channel takes the form of a cylinder with a corrugated surface ("ripples"). In time a broadening of the discharge channel occurs, the depth of the modulation of the discharge radius remaining approximately constant for up to ~30 μsec, after which the modulation depth decreases somewhat during a short interval of time. Then, starting with approximately 40 μsec, highly visible constrictions develop from the "ripples" and the column of plasma loses its regular shape.

The dependence of the diameter of the plasma filament on time was found by a comparator processing of the streak photographs. The processing was run up to approximately 30 μsec, when the shape of the channel allowed the determination of the mean diameter of the cord with an error not exceeding 20%. The time dependence of the visible diameter of the discharge obtained in this way is shown in Fig. 5. As can be seen from the figure, during practically the whole time of the considered phase of the process the visible diameter of the discharge increases at a constant rate on the order of 10^5 cm/sec. The treatment of the streak photographs for different initial voltages across the bank showed that the expansion rate somewhat increases with increase of the initial voltage and, consequently, with the discharge current.

We can calculate the resistance R of the discharge from the volt-ampere characteristics and from the data on the diameter of the discharge filament, using the equation:

$$V = RJ + \frac{d}{dt}(LJ), \qquad (1)$$

where V is the voltage drop across the tube, J is the discharge current, and L is inductance of the tube and obviously depends only on the geometry of the tube and varies with time owing to the variation of the diameter of the plasma filament. Since the discharge tube was not a strictly coaxial system (the outer cylinder was not continuous), the quantity L was found from the experimentally determined calibration of the dependence of L on the diameter of the metallic rods placed between the electrodes. The time dependence of the resistance of a discharge obtained by means of this method is shown in Fig. 6 for V_0 = 20 kV. It can be seen that R decreases substantially in the first 10 μsec. Subsequently, the resistance changes insignificantly and remains of the order of 0.1 Ω.

Let us now turn to the spectral characteristics of a discharge. A typical pattern of the time sweep of the spectrum is shown in Fig. 7. It can be seen that there appears at the beginning of the process a continuous spectrum whose brightness intensifies with growth of the discharge current, the maximum brightness of the continuous spectrum coinciding in time with the peak of

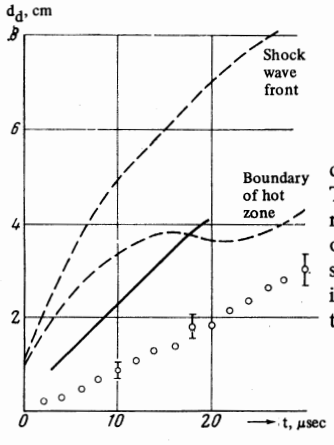

FIG. 5. Time dependence of the diameter of the discharge filament. The points represent experimental results, the solid curve is the result of calculations based on the self-similar theory, and the dashed curve is the result of computer calculations.

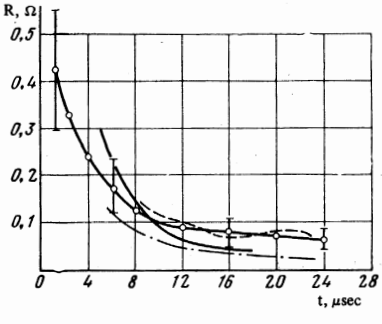

FIG. 6. Dependence of the resistance of a discharge on the time. The points are the results of experiment, the solid curve is the result of a self-similar computation, and the dashed and dash-dot curve—of a computer calculation.

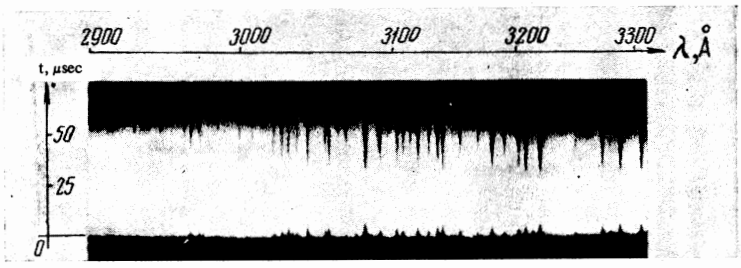

FIG. 7. A section of the time sweep of the spectrum.

the current. Then approximately at 50 μsec a line spectrum appears. It is characteristic that a continuous spectrum is observed practically only in the first half-period and, consequently, it may be supposed that the main part of the energy is radiated in this time interval.

The brightness temperature T of the discharge was determined from the continuous spectrum. Figure 8 shows the dependence of the brightness temperature on wavelength for different moments of time. It follows from this dependence that the brightness temperature of a discharge for the indicated moments of time does not depend on wavelength, i.e., the discharge radiates as a black body in the region from 2000 to 6000 Å. Under the conditions of the experiments the blackness of the radiation in this spectral interval was observed from 10 to 50 μsec, beginning from the moment of breakdown of the discharge gap.

The time dependence of the brightness temperature obtained in this way is shown in Fig. 9 for V_0 = 20 kV in the form of points. It can be seen that the temporal variation of the temperature in the first half-period is qualitatively similar to that of the discharge current. At the maxima of the current the temperature attains values of about 2 eV (1.8 eV at J_{max} = 145 kA and 2.2 eV at J_{max} = 195 kA). A similar behavior of the temperature follows from data given by the photocells. Figure 10 shows typical shapes of the oscillograms of the signals from photocells F-1 (the upper ray) and F-2 (lower ray). Notice that the upper channel of the oscillograph gave a mirror image of the signal. It can be seen from the oscillograms that the brightness of the discharge oscillates like the discharge current. This is especially well noticeable with respect to the shape of the signal from the F-1 photocell (spectral band 3350–4350 Å), and it should be noted that the first main maximum coincides in time exactly with the moment of the first maximum of the current. The second maximum of the brightness corresponds to the second maximum of the current and is much weaker than the first. The oscillogram of the signal from the F-7 photocell, however, practically shows the presence of only the first brightness peak. This attests to the fact that energy is radiated in the ultraviolet band (2350–3300 Å) mainly during the first half-period. Similar qualitative conclusions can be drawn from the analysis of the spectrograms.

It should be noted that in the blackness region the brightness of the discharge (and, consequently, the brightness temperature), determined for the wavelengths λ_1 = 3950 Å and λ_2 = 2800 Å (for wavelengths corresponding to the center of the sensitivity bands of the photocells) from the spectrograms and the characteristics of the photocells coincided to within the limits of the errors of the measurements. In view of this, usually only the spectrographic method, which allowed a detailed investigation of the general nature of the luminescence of a discharge, was used for the determination of the temperature.

It should be noted here, however, that the temperature of a discharge can be calculated from the data on the resistance R and radius of the discharge. Indeed, if we assume that the plasma in the discharge is completely ionized, then we can write for the conductivity of the plasma the well-known expression (see, for example, [1,4]) $\sigma = 10^{14} T^{0.4}$ sec^{-1} (T is given in electron volts), from which it follows that

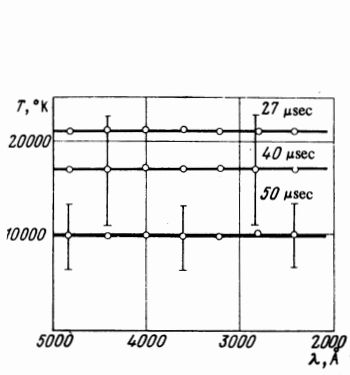

FIG. 8

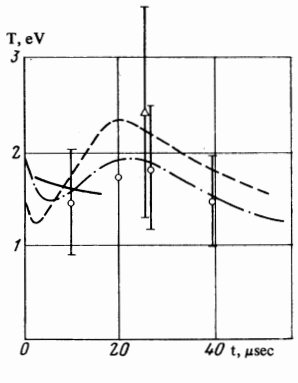

FIG. 9

FIG. 8. Dependence of the brightness temperature of a discharge on wavelength for different moments of time.

FIG. 9. Time dependence of the discharge temperature. The small circles represent the brightness temperature, the triangle is the temperature found from the conductivity of the plasma, the solid curve is the result of a self-similar computation, and the dashed curve the result of a computer calculation.

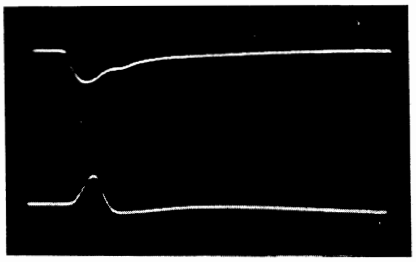

FIG. 10. Typical form of the oscillograms of signals from photocells F-1 (upper ray) and F-7 (lower ray).

$$T^{0,4}(t) = 10^{-14}\frac{e}{R(t)\pi r^2(t)}. \quad (2)$$

According to this relation, the plasma temperature can, generally speaking, be found for different moments of time. However, the error in the determination of T(t) will then be very large. Therefore, the magnitude of T was determined for only the moments of time when dJ/dt = 0, i.e., for the moments of the maxima of the current. The value of the temperature determined in this way is shown in Fig. 9 in the form of a triangle. It can be seen that the value of the temperature computed from the plasma conductivity is in good agreement with the brightness temperature of the discharge.

Let us estimate the energy balance in a discharge. Figure 11 shows the dependence on time of the energy expended on the discharge

$$Q = \int_0^t I^2 R dt \quad (3)$$

and of the energy radiated in definite spectral bands ($\Delta\lambda = \lambda_2 - \lambda_1$):

$$W_{\Delta\lambda} = 2\pi l \int_0^t \int_{\lambda_1}^{\lambda_2} r(t) S_{\lambda p}(t)\, dt\, d\lambda, \qquad S_{\lambda p} = 2\pi h c^2 \lambda^{-5}[e^{hc/\kappa T\lambda} - 1]^{-1}, \quad (4)$$

where $S_{\lambda p}$ is the spectral flux of the radiation of an absolutely black body, and l is the length of the discharge. These curves were constructed for the first quarter of the period of the discharge, since only for this section of the time can we speak of a cylindrical shape of the discharge channel with sufficient degree of accuracy. The triangle denotes the value of the internal energy of the discharge at the moment the current attains its maximum value, $U = (1 + z)N\kappa T\pi R^2 l$, while the square represents the energy which has gone into the ionization of the air enveloped by the heat wave. It was assumed in the calculation that there occurs during the expansion of the discharge channel a complete capture of particles into the discharge with the unperturbed density, $N = 2.7 \times 10^{19}$ cm^{-3}, corresponding to normal conditions. The quantity z was taken from tables,[19] and the mean ionization potential was assumed equal to 13 eV.

Let us now proceed to the comparison of the energy liberated and dissipated in the plasma, taking note at once that, since the plasma column expands in the entire considered phase of the process, the work done by the ponderomotive forces can be neglected and the total energy evolved in the plasma is equal to Q. Then the energy balance in the discharge can be written in the form

$$Q = W_{\Delta\lambda_2} + U + I + E_{kin}, \quad (5)$$

where E_{kin} is the kinetic energy of the plasma, which can be estimated using the usual formula $mv^2/2$, where m is the mass of the gas enveloped by the discharge channel, and v is the rate of its expansion. Under our conditions, $E_{kin} = (1-2)\times 10^2$ J, i.e., it is negligibly small. It is natural to take as $W_{\Delta\lambda_2}$ the energy emitted in the transparency band of air ($\lambda_2 = \infty$, $\lambda_1 = 1860$ Å). It was also assumed in the calculation that the discharge radiated like a black body in the entire indicated spectral range. As follows from the data shown in Fig. 11, the energy expended on the discharge up to the moment of the current peak is equal in this case to ~17 kJ, while the energy dissipated is $(W_{\Delta\lambda_2} + U + I) \approx (4 + 3.5 + 10)$ kJ = 17.5 kJ, i.e., there is an excellent quantitative agreement. For an initial charging voltage V_0 = 24 kV, the corresponding quantities are equal to 31 and (9.5 + 6.5 + 17) = 33 kJ.

In view of the estimates made above, it is clear that it is incorrect to neglect the ionization energy in the energy balance of a discharge, as was done in [11].

It follows from the above-cited results that during the first quarter of the period of the current ~30 and ~37% of the energy stored in the bank (for charging voltages V_{01} = 20 kV and V_{02} = 24 kV, respectively) is expended on a discharge. During the same period of time, ~24% of the energy expended on the discharge and ~7% of the stored energy for the case V_{01} and, 31 and 12% for the cases V_{02}, are radiated in the transparency band of the air. It follows from these figures that the discharge converts the stored energy efficiently into radiation energy.

Figure 11 also shows curves for the energy $W_{\Delta\lambda_1}$ radiated in the entire spectral band $\lambda_2 = \infty$, $\lambda_1 = 0$. These curves were plotted using formula (4) and the data on the brightness temperature, and for the energy $W_{\Delta\lambda_3}$ radiated in the ultraviolet region ($\lambda_1 = 2200$ Å, $\lambda_2 = 2700$ Å). The latter characterizes the discharge from the point of its use as a source of ultraviolet radiation. It can be seen that in this region ~1.1 kJ is evolved in the first case and ~2.2 kJ in the second.

It follows from the observed nature of the development of the discharge that the foregoing data on the expended and radiated energies can be extrapolated to the entire half-period by simply doubling them, it being clear that such an extrapolation will give underestimated results. This is especially true of the values of W, since the temperature curves are approximately symmetrical about the peak of the current whereas the radius of the discharge increases continually. Proceeding in this fashion, we find that for a charging voltage V_{01} = 20 kV during the first half-period τ = 54 μsec, ~35 kJ (~60% of the stored energy $\mathscr{E}$) are expended on the discharge, ≳9 kJ (≳15% of $\mathscr{E}$) are radiated in the transparency band of air, and ≳2.2 kJ (≳4%) are radiated in the ultraviolet region. For the case V_{02} = 24 kV, the corresponding values are ~60 kJ (≳75% of $\mathscr{E}$), ≳20 kJ (≳25%), and ≳4.4 kJ (≳5%).

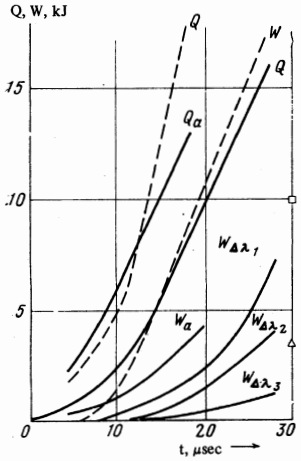

FIG. 11. Energy characteristics of a discharge (V_0 = 20 kV): Q is the energy expended on the discharge, $W_{\Delta\lambda}$ the radiation energy in different spectral bands ($\Delta\lambda_1$: $0 < \lambda < \infty$; $\Delta\lambda_2$: 1860Å $< \lambda < \infty$: $\Delta\lambda_3$; 2460Å $< \lambda <$ 2860Å), the small circles are experimental values, the solid curves the results of self-similar computations, and the dashed curves are the results of computer calculations. Δ represents the internal energy of the plasma, and □ the energy necessary for the ionization of the gas drawn into the discharge.

Thus, up to 75% of the stored energy is injected into the plasma in the first half-period, up to 25% of $\mathcal{E}$ being radiated in the transparency window of air and up to 5% in the ultraviolet band 2200–2700 Å.

Finally, we give the results of the measurement of the energy radiated during the entire process, obtained with the aid of a calorimeter, and corresponding to the transmission band of quartz (up to ~2000 Å). This energy is equal to 26 kJ or 45% of $\mathcal{E}$ for the case V_{02} = 20 kV, and 38 kJ or 42% of $\mathcal{E}$ for the case V_{02} = 24 kV, i.e., the discharge converts electrical into light energy efficiently.

4. COMPARISON OF THE EXPERIMENTAL RESULTS WITH THEORY

The only method available up till now for the analytical description of the processes that occur in heavy-current discharges in gases under high pressures is the self-similar solution of the equations of magnetohydrodynamics with radiant thermal conduction, obtained in [7]. However, this solution was obtained under quite a number of simplifying assumptions which lead, as shown in [12], to a limitation on the region of its applicability to a definite time interval. For the case when the current varies linearly with the time (J = Ft), the region of applicability is defined by the inequality

$$t_1 = \frac{3.5}{F^{1,17}} < t < \frac{17}{F^{1,05}} = t_2, \qquad (6)$$

where F is the rate of growth of the current in units of 10^{10} A/sec, and t is the time measured from the beginning of the process in μsec. We note that, as follows from the oscillograms of Fig. 3, we can, with a sufficient degree of accuracy, assume the growth of the current in our experiments to be linear—with $F_1 = 0.7 \times 10^{10}$ A/sec for V_{01} = 20 kV and $F_2 = 1 \times 10^{10}$ A/sec for V_{02} = 24 kV, which corresponds to approximate time intervals $(t_2 - t_1)$ 5–25 μsec and 3.5–17 μsec, respectively. Thus, the initial stage of the process in our experiments was sufficiently extended in time to allow it to be described by the self-similar theory.

According to the self-similar theory, it is easy for the case of a discharge in air, when J = Ft, to obtain the following expressions for the diameter of the discharge channel (the diameter of the thermal wave) d_p, the temperature T, the resistance R, the energy Q expended on the discharge, and the energy $W_{\Delta\lambda_1}$ radiated in the entire spectral range $0 < \lambda < \infty$ (per centimeter of length):

$$d_p(t) = 3.84 \cdot 10^{4} F^{0,33} t^{0,835} \text{ (cm)}, \qquad (7)$$

$$T(t) = 1.05 F^{0,34} t^{-0,033}, \qquad (8)$$

$$R(t) = 7.6 \cdot 10^{-12} F^{0,8} t^{-1,66} \text{ (}\Omega\text{)}, \qquad (9)$$

$$Q(t) = 5.2 \cdot 10^{8} F^{1,2} t^{1,34} \text{ (J)}, \qquad (10)$$

$$W_{\Delta\lambda_1}(t) = 7.55 \cdot 10^{9} F^{1,69} t^{1,703} \text{ (J)}, \qquad (11)$$

where F is expressed in units of 10^{10} A/sec, and t is in sec. It was assumed in the derivation of the expression (11) that the discharge radiated like an absolutely black body of temperature T (an assumption which is the basis of the self-similar computation).

The curves computed from the formulas (7)–(11) are shown in Fig. 5, 6, 9, and 11 as solid lines (without points). Comparison of these curves with the experimental curves shows that the self-similar theory correctly describes the temporal behavior of all the quantities, with the exception of the temperature: the quantity T grows with the time at the initial stage, whereas the self-similar theory predicts a slow decrease of the temperature. The same result has been noted earlier. [11,12] As for the quantitative comparison, the calculated values of the diameter of the discharge channel and the energy quantities Q and $W_{\Delta\lambda_1}$ for the small rate of injection of energy into the discharge, $F_1 = 0.7 \times 10^{10}$ A/sec (V_{01} = 20 kV), considerably (almost by a factor of two) exceed the experimental values, while for $F_2 = 1 \times 10^{10}$ A/sec (V_{02} = 24 kV) they are in good quantitative agreement (remaining, to be sure, higher than the experimental values). The temperature T computed from the self-similar theory is in good agreement with the mean value of T in the first half-period of the current, obtained from the spectrograms. It should also be noted that, as follows from Fig. 11, ~25% of the injected energy is, according to the self-similar theory, radiated before the moment of time t_2 in the entire spectral band of $W_{\Delta\lambda_1}$. This is in good agreement with the estimate from the experimental data, which yields for up to the same moment of time the corresponding value of 20%. Thus, it is possible to carry out with the aid of the self-similar theory accurate semiquantitative calculations of the principal characteristics of a discharge, in particular, of the energy and light characteristics, the accuracy of these calculations increasing with increase of the rate of growth of the current (rate of energy input).

The main defect of the self-similar theory, as has already been noted above, is the neglect of a number of factors, the most important of which is the action of the self-magnetic field on the discharge. It is precisely the neglect of the magnetic pressure of the discharge current in comparison with the gas kinetic pressure that leads to the presence of the time limit t_2. In view of this, an attempt was made to describe the entire discharge process as a whole with the aid of electronic computer calculations.[1)]

A numerical solution of the equations of magnetohydrodynamics with allowance for radiative transport of heat was carried out:

$$\frac{\partial v}{\partial t} = -r\frac{\partial P}{\partial x} + F, \; F = -\frac{j_z H_\varphi}{\rho}, \; \frac{\partial r}{\partial t} = v,$$

$$\frac{\partial}{\partial t}\left(\frac{1}{\rho}\right) = \frac{\partial (rv)}{\partial x}, \; \frac{\partial}{\partial t}\left(\frac{H_\varphi}{\rho r}\right) = \frac{\partial E_z}{\partial x},$$

$$j_z = \sigma E_z, \; E_z = \frac{\rho}{4\pi\sigma}\frac{\partial (rH_\varphi)}{\partial x},$$

$$\frac{\partial \varepsilon}{\partial t} = -P\frac{\partial (rv)}{\partial x} + Q + \frac{\partial S}{\partial x}, \; Q = \frac{j_z E_z}{\rho},$$

$$\sqrt{1-\gamma^2}\left(\mu\frac{\partial I}{\partial r} + \frac{1-\mu^2}{r}\frac{\partial I'}{\partial \mu}\right) + \varkappa' I' = \frac{1}{\pi}\hat{\sigma}T^4,$$

$$S = 2\int_0^1 \sqrt{1-\gamma^2}\, d\gamma \int_{-1}^{+1} \mu I' d\mu / \sqrt{1-\mu^2}, \qquad (12)$$

[1)] The methods used in the problems of radiation magnetohydrodynamics were worked out at the Institute of Applied Mathematics of the USSR Academy of Sciences by a group led by A. A. Samarskiĭ. V. Ya. Gol'din, N. N. Kalitkin, S. P. Kurdyumov, Yu. P. Popov and B. N. Chetverushkin participated in these investigations. A detailed exposition of the methods and calculations has been published in [29].

where r is the Euler coordinate (radius), ρ the density of the medium, x ($dx = \rho r\, dr$) the Lagrange mass coordinate, P the gas-kinetic pressure, F the ampere force, H_φ the azimuthal component of the intensity of the magnetic field of the discharge current, v the radial component of the velocity, E_z and j_z—the longitudinal (axial) components of the electric field strength and current density, ϵ the internal energy, σ the electrical conductivity, Q the Joule heating, S the radiation energy flux, $\hat{\sigma}$ the Stefan-Boltzmann constant, κ' the coefficient of absorption of radiation with allowance for re-emission, and $I'(\mu, \gamma, r, t)$ the intensity of radiation, and γ and μ the cosines of the angles between the axes r and z and a prescribed direction (the direction of photon emission).

The calculation of the radiation was carried out on the basis of the transport equation for the radiation averaged over the spectrum.

It was assumed in the solution that the discharge occurs in some finite cylindrical region of the gas and therefore the solution was sought in the intervals $t > 0$ and $0 \leq x \leq m$, where m is the mass of the gas per unit height of the discharge and one radian of the azimuthal angle φ. The boundary conditions were formulated in the following manner: the motion of the gas was assumed to be bounded from the right at x = m by the rigid wall of the discharge chamber:

$$v(m, t) = 0, \tag{13}$$

and a radiation flux from outside was assumed to be nonexistent:

$$I'(\mu > 0, \gamma, m, t) = 0. \tag{14}$$

The boundary conditions for the electromagnetic field were determined with the aid of the equation of an external circuit:

$$r(m, t) H_\varphi(m, t) = 2J(t),$$
$$L_0 \frac{dJ}{dt} + R_0 J - V_0 + \frac{1}{C_0}\int_0^t J(t)\,dt - E(m, t) = 0, \tag{15}$$

where, as before, J is the discharge current; L_0 and R_0 are the stray inductance and resistance of the discharge circuit, C_0 is its capacitance, and V_0 is the initial voltage across the capacitor bank; all the quantities pertain to a unit length of the discharge.

The computation was carried out for $V_0 = V_{01}/l$ (V_{01} = 20 kV, and l = 75 cm) and for the stray parameters corresponding to the inclusion of the capacitances C_1 and C_2 of the discharge circuit employed. The boundary of the discharge region was chosen to correspond to the radius of the circle around which the rods forming the return conductor were arranged in the experiment.

The fulfilment of the conditions:

$$v(0, t) = 0,\ H_\varphi(0, t) = 0,\ S(0, t) = 0. \tag{16}$$

arising from the symmetry of the problem, was required on the axis of the discharge.

Before formulating the initial conditions, we must make a few remarks. They concern the role of the material of the thin wire which is used to trigger the breakdown of the long discharge gap. Naturally, in a rigorous analysis we must take into account in the computations such processes as the warming up of the thin wire by the current, phase transitions (the melting and evaporation of the fused metal, or sublimation), the creation of conditions for a subsequent breakdown of the vapor of the metal, the ionization of the surrounding gas, and the heating of it to sufficiently high temperatures. It is these processes that lead in the long run to the production of a column of a fully ionized plasma, for whose description the magnetohydrodynamic approach is valid. It is not difficult to understand that it is simply impossible to take all the above-enumerated factors into account, owing to the complexity of the phenomena. However, under our conditions, this was not necessary, since, as the experiments showed, it is possible to choose conditions (the material of the thin wire and its diameter) such that the principal parameters of the discharge (radius, temperature) practically do not depend on the initial conditions. Therefore, the following was chosen as the initial state: a narrow temperature peak around the axis of the discharge gap in a general cold (room temperature) background of constant initial gas density (2.7×10^{19} cm^{-3}). There remains, however, in that case an arbitrariness in the choice of the radius r_0 and the temperature T_0 of this peak. These quantities were varied. The gas was considered to be air. Its conductivity σ was calculated in accordance with the results of [21]; data on the absorption coefficient and the equation of state were taken from tables.[19]

The system of equations (12) was approximated in the numerical computations by a homogeneous, completely conservative difference system, which was further solved by the successive sweep method with iterations.[22 23] The methods expounded in [24,25] were used in the numerical integration of the transport equation. The electrotechnical equation was solved together with the electromagnetic field equations by a noniterative method.[26]

The results of the numerical computations are shown in Figs. 3, 5, 6, 9, and 11 as dashed and dot-dash curves. The dashed curves correspond to T_0 = 1.5 eV, r_0 = 0.5 cm, while the dot-dash curves correspond to T_0 = 2 eV, and r_0 = 0.8 cm. Comparison of the theoretical and experimental curves shows that, under our assumptions, a computer calculation allows a good quantitative description of the volt-ampere characteristics of the discharge (this is not possible with the self-similar theory) and of the behavior of the temperature. As for the other parameters of the discharge, a computer calculation yields roughly the same disagreement with experiment as the self-similar theory, with this important difference that the calculation describes the entire process at all stages. We could have demanded a better quantitative agreement, but under the simplifications made (especially, concerning the allowance for radiation and the processes of ionization of the gas), even a computer calculation cannot, apparently, yield a high accuracy.

5. MAIN CONCLUSIONS

The experiments and computations show that we can, with the aid of an electric explosion of conductors in air, produce a long-lasting stable state of a discharge, in which the zone encompassed by the thermal wave grows steadily at a rate on the order of 10^5 cm/sec. The temperature of the radiating surface of the discharge varies in conformity with the variation of the discharge current within the limits, from 1.5 to 2 eV, in the principal phase

Characteristics of the different sources of radiation for laser pumping

Type of pumping source	IFP-5000	Flash lamp "Sovet" UF 900/20	Lithium discharge in a vacuum (FIAN)	Explosion in air 20 kV	Explosion in air 24 kV
Length of discharge l (cm)	25	90	14.5	75	75
Duration of principal phase of discharge τ (μsec)	620	150	70	55	55
Energy of the bank & (kJ)	5	20	26.5	58	83
Total energy fed into discharge Q(kJ)	4	16	17.5	35	60
Brightness temperature at the peak T(°K)	9000	11000	17000	21000	26000
Energy radiated in the band 1860A $< \lambda < \infty$, $W_{\Delta\lambda_3}$ (kJ)	—	—	—	9	20
Energy radiated in the band 2200A $< \lambda <$ 2700A, $W_{\Delta\lambda_2}$ (kJ)	0.2	1.0	1.03	2.2	4.4
Total energy radiated (2000A $< \lambda < \infty$) W (kJ)	2.6	—	6.7	26	38
Conversion coefficient η = W/& (%)	50	—	25	45	45
Conversion coefficient in the ultraviolet region $\eta_{\Delta\lambda_3} = W_{\Delta\lambda_3}/\&$ (%)	4	5	4	4	5

of the process which corresponds to the first half-period of the discharge current. For the parameters of the experimental setup used, an efficient conversion of the stored energy into discharge energy takes place (~70% of the stored energy is converted into discharge energy during the first half-period). The energy injected into the discharge is, in its turn, efficiently converted into light energy.

The characteristics of the discharge, from the point of view of its use as a source of radiation for laser pumping, are given in the table. The data pertaining to the xenon lamps and lithium discharge were taken from [8,9,27,28]. As can be seen, a discharge in air has roughly the same efficiency of conversion of energy into radiation in the ultraviolet band (~(4–5)%) as the other existing sources, but its absolute yield of radiation in this band is higher by an order of magnitude. Moreover, the investigated discharge radiates in the transparency band of air more than 40 kJ or more than 45% of the stored energy. The quoted figures show a high efficiency of and prospects for the use of discharges in gases for power pumping of lasers, especially in the ultraviolet region.

[1] V. B. Rozanov and A. A. Rukhadze, Review Report at the 9th International Conference on Phenomena in Ionized Gases, Bucharest, 1969.

[2] A. F. Aleksandrov, A. A. Rukhadze, and S. A. Triger, Transactions of the 9th International Conference on Phenomena in Ionized Gases, Bucharest, 1969.

[3] A. F. Aleksandrov, A. A. Rukhadze, and S. A. Triger, in: Voprosy fiziki nizkotemperaturnoi plazmy (Problems in Low-temperature Plasma Physics), Nauka i Tekhnika, Minsk, 1970.

[4] A. A. Rukhadze and S. A. Triger, Prikl. Mekh. Teor. Fiz. No. 3, 11 (1968).

[5] V. B. Rozanov, A. A. Rukhadze, and S. A. Triger, Prikl. Mekh. Teor. Fiz. No. 5, 18 (1968).

[6] A. A. Rukhadze and S. A. Triger, Zh. Eksp. Teor. Fiz. 56, 1029 (1969) [Sov. Phys.-JETP 29, 553 (1969)]; Zh. Tekh. Fiz. 40, 1817 (1970) [Sov. Phys.-Technical Physics 15, 1418 (1971)].

[7] N. G. Basov, B. P. Borovich, V. S. Zuev, V. B. Rozanov, and Yu. Yu. Stoĭlov, Zh. Tekh. Fiz. 40, 805 (1970) [Sov. Phys.-Technical Physics 15, 624 (1970)].

[8] A. D. Klementov, G. V. Mikhaĭlov, F. A. Nikolaev, and V. B. Rozanov, Transactions of the 9th International Conference on Phenomena in Ionized Gases, Bucharest, 1969.

[9] A. D. Klementov, G. V. Mikhaĭlov, F. A. Nikolaev, V. B. Rozanov, and Yu. P. Sviridenko, Teplofizika Vysokikh Temperatur 8, 736 (1970) [Sov. Journ.-High Temperature 8, 698 (1970)].

[10] A. F. Aleksandrov, V. V. Zosimov, A. A. Rukhadze, and V. S. Savoskin, Kratkie soobshcheniya po fizike (Short Communications on Physics) Izd. FIAN, No. 6, 58 (1970).

[11] N. G. Basov, B. P. Borovich, V. S. Zuev, V. B. Rozanov, and Yu. B. Stoĭlov, Zh. Tekh. Fiz. 40, 516 (1970) [Sov. Phys.-Technical Physics 15, 399 (1970)].

[12] A. F. Aleksandrov, V. V. Zosimov, A. A. Rukhadze, V. I. Savoskin, and I. B. Timofeev, Kratkie coobshcheniya po fizike (Short Communications on Physics), FIAN, No. 8, 72 (1970).

[13] L. A. Artsimovich, Upravlyaemye termoyadernye reaktsii (Controlled Thermonuclear Reactions), Fizmatgiz, 1961 (Eng. Ed., Gordon & Breach, New York, 1964).

[14] V. F. D'yachenko and V. S. Imshennik, in: Voprosy teorii plazmy, pod red. M. A. Leontovicha (Problems of Plasma Theory; Editor, M. A. Leontovich), Vol. 5, Atomizdat, 1967.

[15] Tekhnika bol'shikh impul'snykh tokov i magnitnykh poleĭ (The Techniques of Heavy Pulsed Currents and Magnetic Fields; Editor, V. S. Komel'kov), Atomizdat, 1970.

[16] N. N. Ogurtsova, I. V. Podmoshenskiĭ, and V. M. Shelemina, Optika i Spektroskopiya 16, 949 (1961) [Optics and Spectroscopy 16, 514 (1964)].

[17] Exploding Thin Wires (Russian Transl. Edited by A. A. Rihadze, IIL, 1963).

[18] Electric Explosion of Conductors (Russian Transl. Edited by A. A. Rukhadze, and I. S. Shpigel', "Mir," 1965).

[19] N. M. Kuznetsov, Termodinamicheskie funktsii i udarnye adiabaty vosdukha pri vysokikh temperaturakh (Thermodynamic Functions and the Impact Adiabats of Air at High Temperatures), Mashionostroenie, M., 1965.

[20] Ya. B. Zel'dovich and Yu. P. Raĭzer, Fizika udarnykh voln i vysokotemperaturnykh gidrodinamicheskikh yavleniĭ (The Physics of Shock Waves and High-temperature Hydrodynamic Phenomena), Fizmatgiz, 1963 (Eng. Transl. Academic Press, New York, 1966).

[21] N. N. Kalitkin and V. S. Rogov, in: Voprosy fiziki nizkotemperaturnoĭ plazmy (Problems of Low-temperature Plasma Physics), Nauka i Tekhnika, Minsk, 1970.

[22] Yu. P. Popov and A. A. Samarskiĭ, Zh. Vychislit. Mat. Fiz. 8, 990 (1968).

[23] A. A. Samarskiĭ, P. P. Volosevich, M. I. Volchinskaya, and S. A. Kurdyumov, Zh. Vychislit. Mat. Fiz. 8, 1025 (1968).

[24] V. Ya. Gol'din, G. V. Danilova, and B. N. Chetverushkin, in: Vychislitel'nye metody v teorii perenosa (Computational Methods in Transport Theory), Atomizdat, 1964.

[25] B. N. Chetveryshkin, Zh. Vychislit. Mat. Fiz. 10, No. 5 (1970).

[26] Yu. P. Popov, Zh. Vychislit. Mat. Fiz. 11, 449 (1971).

[27] A. D. Klementov and G. V. Mikhaĭlov, Zh. Priklad. Spektrosk. 9, 756 (1968).

[28] A. A. Vekhov, G. V. Mikhaĭlov, F. A. Nikolaev, and Yu. P. Sviridenko, Zh. Priklad. Spektrosk. 12, 979 (1970).

[29] V. Ya. Gol'din, N. N. Kalitkin, S. P. Kurdyumov, Yu. P. Popov, A. A. Samarskiĭ, and B. N. Shetverushkin, Preprint, Institute of Applied Mathematics, USSR Academy of Sciences, No. 2 (1971).

Translated by A. K. Agyei
192